

# Fragmentation of rods by cascading cracks: why spaghetti do not break in half

Basile Audoly and Sébastien Neukirch

*Lab. de Modélisation en Mécanique, CNRS/UPMC, 4 place Jussieu, Paris, France.*

(Dated: December 22, 2004)

When thin brittle rods such as dry spaghetti pasta are bent beyond their limit curvature, they often break into more than two pieces, typically three or four. With the aim to understand these multiple breakings, we study the dynamics of a rod bent just below its limit curvature and suddenly released at one end. We find that the sudden relaxation of the curvature at the newly freed end leads to a burst of flexural waves, whose dynamics are described by a self-similar solution with no adjustable parameters. These flexural waves locally *increase* the curvature in the rod and we argue that this counter-intuitive mechanism is responsible for the fragmentation of brittle rods under bending. A simple experiment supporting the claim is presented.

PACS numbers: 62.20.Mk, 46.50.+a, 46.70.De

The physical process of fragmentation is relevant to several areas of science and technology. Because different physical phenomena are at work during the fragmentation of a solid body, it has mainly been studied from a statistical viewpoint [1–5]. Nevertheless a growing number of works have included physical considerations: surface energy contributions [6], nucleation and growth properties of the fracture process [7], elastic buckling [8, 9], and stress wave propagation [10]. Usually, in dynamic fragmentation, the abrupt application of fracturing forces (e.g. by an impact) triggers numerous elementary breaking processes, making a statistical study of the fragments sizes possible. This is opposed to quasi-static fragmentation where a solid is crushed or broken at small applied velocities [11]. Here we consider such a quasi-static experiment whereby a dry spaghetti is bent beyond its limit curvature. This experiment is famous as, most of the time, the pasta does not break in half but typically in three to ten pieces. In this Letter, we explain this multiple failure process and point out a general mechanism of cascading failure in rods: a breaking event induces strong flexural waves which trigger other breakings, leading to an avalanche like process.

Let us consider a rod which is held at both ends and bent quasi-statically with an increasing, uniform curvature. It breaks at time  $t = 0$  when its curvature  $\kappa_0$  reaches its limit value  $\kappa^*$ : a dynamic crack crosses the weakest section and breaks the rod in two halves. As the rod was initially bent with uniform curvature, the location of this first failure point is that of the strongest defect. We shall not further discuss this initial breaking event, but instead focus on the subsequent dynamics of either half of the rod, for  $t > 0$ , and show that this dynamics generically leads to new breaking events at later times.

Since we are not interested in the statistics of the initial breaking event, we introduce and analyze throughout this Letter a model problem in which *the release of a rod mimics the initial breaking event*. Both problems indeed obey the same equations but the advantage of the model

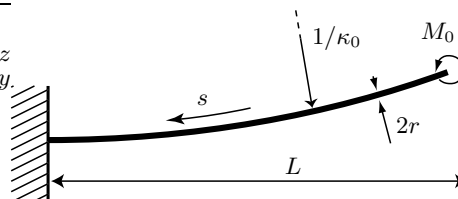


FIG. 1: The dynamics of a rod fragment following the initial breaking event in a brittle rod is modelled by releasing at time  $t = 0$  a rod with fixed length  $L$ , initial curvature  $\kappa_0$  and no initial velocity.

problem is that the length  $L$  of the fragment is known in advance. In the model problem, the rod is initially uniformly bent and at rest. This is achieved by clamping one end and applying a moment  $M_0$  at the other end:  $M_0$  plays the role of the internal moment transmitted across the section that is about to fail, see Fig. 1. At time  $t = 0$ , this end is suddenly released as the applied moment  $M_0$  is removed instantaneously. The rod no longer is in equilibrium and we study its subsequent dynamics.

The dynamics of thin rods are described by the celebrated Kirchhoff equations [12] which in the limit of small planar oscillations take the form:

$$L^4 \kappa_{,s^4}(s, t) + T^2 \kappa_{,t^2}(s, t) = 0, \quad (1)$$

where a comma in indices denotes a partial derivative. Here, we have introduced a typical time  $T$  built from the rod mechanical properties:  $T = L^2/\gamma$  where  $\gamma = \sqrt{EI/(\rho A)}$ , with  $E$  the Young's modulus,  $\rho$  the mass density,  $A$  the area and  $I$  the principal moment of inertia of the cross section. For a rod with circular cross section of radius  $r$ ,  $I = \pi r^4/4$  and  $\gamma = cr/2$ , where  $c = \sqrt{E/\rho}$  is the sound velocity in the material. Note that  $T$  is directly proportional to the period of the fundamental mode of free oscillations of the rod [13],  $T_{\text{free}} = 1.79 T$ .

Equation (1) calls for some remarks. First, we are only interested in planar configurations of the rod. Consequently the geometry of the rod at any time  $t$  is parameterized by a single unknown function, its curvature

$\kappa(s, t)$  as a function of its arc-length  $s$ . Second, we have introduced the equations for rods in the limit of small oscillations, which can seem a rather restrictive assumption. The purpose is merely to avoid unessential computational difficulties in the presentation. In fact, we did take these nonlinearities into account in the numerical simulations presented below. Third, the small amplitude oscillations of a rod are classically studied in terms of the transverse displacement  $y(s, t)$ . Here, the important variable which is connected to the failure of the rod in flexion is the curvature  $\kappa(s, t)$ , which was therefore chosen as the unknown in Eq. (1).

On Eq. (1), we impose clamping conditions at  $s = L$ :  $\kappa_{,s^2}(L, t) = 0$ ,  $\kappa_{,s^3}(L, t) = 0$ , and free boundary conditions at  $s = 0$ :  $\kappa(0, t) = 0$ ,  $\kappa_{,s}(0, t) = 0$ . These four boundary conditions in  $s$  associated with the two initial conditions  $\kappa(s, 0) = \kappa_0$  and  $\kappa_{,t}(s, 0) = 0$  (uniform curvature  $\kappa_0$ , no initial velocity) warrant, in principle, a unique solution  $\kappa(s, t)$  to Eq. (1).

A key remark must be made here, which is at the heart of the rich dynamics of the released rod. These initial and boundary conditions are inconsistent: the curvature  $\kappa(0, t)$  at the free end has to be  $\kappa_0 \neq 0$  at initial time  $t = 0$ , while the free end condition requires that it vanishes at any time  $t > 0$ . This inconsistency can be understood easily: the initial configuration with uniform curvature  $\kappa_0$  violates the constitutive relation of the rod (the curvature is proportional to the internal moment, even in the dynamic theory of rods) and must therefore vanish near a free end. This is a typical boundary layer situation: the assumptions underlying the derivation of the Kirchhoff equations break down in some domain where the solution is sought (here, at small times and in the vicinity of the free end) — an example of a boundary layer arising for similar reasons in a static problem is the eversion of an elastic ball [14]. A detailed analysis of this boundary layer will be presented in a separated paper [15]. Here, it is sufficient to remark that in order to solve this boundary layer, one has to restore in one way or another the small thickness  $r$  of the rod into the equations — for instance by taking into account the finite time needed for the initial crack to propagate through a cross-section of the rod, leading to a decrease of  $M_0$  over a small but finite timescale  $T_s = r/c \sim 1 \mu\text{s}$  for spaghetti, where  $c$  is the typical speed of propagation of the transverse dynamic crack. Being based on the length-scale  $r$ , this boundary layer characterizes the rod dynamics over typical times  $T_s$  and in a region of size  $\sim r$  around the free end. The ratio of this timescale to the ‘macroscopic’ timescale introduced before reads  $T/T_s = 2(L/r)^2$ , that is the square of the (large) aspect ratio of the rod. Since  $L/r \sim 250$  for spaghetti pasta, there are three to four orders of magnitude between  $T_s$  and  $T$ . As long as one is not interested in describing the dynamics of the rod over timescales as short as  $T_s$ , one can disregard the details of this boundary layer.

The inconsistency in the boundary and initial condi-

tions of Eq. (1) is therefore solved by noticing that the initial curvature  $\kappa(L, t)$  relaxes from its initial value,  $\kappa_0$ , to zero over the short timescale  $T_s \lll T$ . This simple remark has two crucial consequences. First the relaxation of  $\kappa(L, t)$ , being very abrupt, generates a burst of flexural waves which are strong enough to break the rod, as we explain below. Second, the separation of scales  $T_s \lll T$  can be utilized to derive an analytic solution to our problem in the so-called intermediate asymptotic regime

$$T_s \ll t \ll T \quad (2)$$

which we study here. Solutions of the regularized problem are indeed described in the limit  $t \gg T_s$  by self-similar solutions [16]. Owing to the obvious scaling  $s \sim L \sqrt{t/T}$ , we seek a solution of Eq. (1) in the form  $\kappa(s, t) = \kappa_0 u(\xi)$ , where the self-similarity variable is  $\xi = (s/L)/\sqrt{t/T} = s/\sqrt{\gamma t}$ . Note that we have factored out the initial curvature  $\kappa_0$ , as we discuss the small amplitude limit of the Kirchhoff equations [17]. The boundary conditions for  $u(\xi)$  are derived from those for  $\kappa$ :  $u(0) = 0$ ,  $u'(0) = 0$  and  $u(+\infty) \rightarrow 1$ . Substituting this self-similar form of  $\kappa(s, t)$  into Eq. (1) yields the following equation for the self-similar solution  $u(\xi)$ :

$$4 u''''(\xi) + \xi^2 u''(\xi) + 3 \xi u'(\xi) = 0 \quad (3)$$

Imposing that  $u(\xi)$  tends toward a constant for  $\xi \rightarrow +\infty$  implies that  $u''(0) = 0$ , as shown with the help of an integral of motion. This last condition, in addition to the previous ones, yields a *unique* self-similar solution to Eq. (3):

$$\kappa(s, t) = 2\kappa_0 S \left( \frac{1}{\sqrt{2\pi}} \frac{s}{\sqrt{\gamma t}} \right), \quad (4)$$

where we have introduced the Fresnel sine integral,  $S(x) = \int_0^x \sin(\frac{\pi}{2} y^2) dy$ , arising in diffraction theory. Equation (4) does not describe a progressive wave with constant velocity,  $s \sim ct$ , but instead a self-similar solution  $s \sim \sqrt{\gamma t}$ . This reflects the dispersive nature of Eq. (1).

Bent rods that are suddenly released at one end are all described in the intermediate regime (2) by the same universal solution (4) independently of the material properties, of the details of the initial release or breaking (as long as they take place over a short timescale  $T_s \lll T$ ) and even of the boundary conditions imposed at the other end  $s = L$ , which have not been used to derive Eq. (4). This universal solution is plotted in Fig. 2, bottom, along with a numerical solution of the Kirchhoff equations — including nonlinearities omitted in Eq. (1). This numerical solution features, as expected, the self-similar regime for  $T_s \ll t \ll T$  in which a burst of flexural waves emitted from the released end  $s = 0$  travels along the rod with a square root time dependence. The self-similar solution (4) accurately describes the rod dynamics until reflections on the clamped end  $s = L$  take place, for

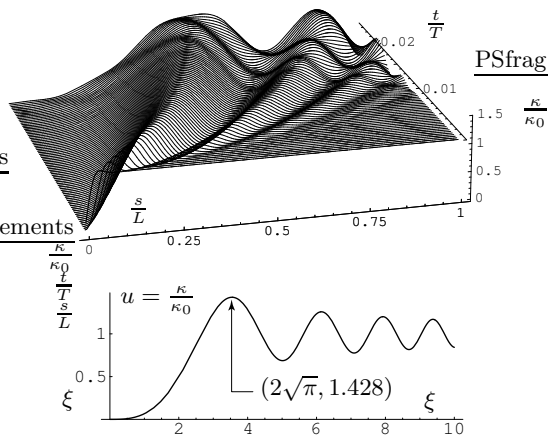


FIG. 2: *Top*: numerical solution of the nonlinear Kirchhoff equations for an initial half-circle configuration,  $\kappa_0 = \pi/L$ . The curvature at the free end  $\kappa(0, t)$  relaxes to zero within the first few time steps (inner solution of the boundary layer problem) while it is given in the intermediate regime (2) by the universal self-similar solution (4) (outer solution). At later times, for  $t \sim T$ , reflections take place on the clamped end  $s = L$ . *Bottom*: self-similar solution describing the intermediate regime with  $\xi = s/\sqrt{\gamma t}$ .

$t \sim T$ . At these large times, the rod dynamics can be obtained by numerical integration of the Kirchhoff equations using the self-similar solution (4) as initial value. This self-similar solution being universal, the behaviour of the rod at long times remains universal (it only depends on the boundary condition at  $s = L$ ).

A key property of the self-similar solution (4) is that the curvature  $\kappa(s, t)$  is locally significantly *larger* than the initial curvature  $\kappa_0$ . Indeed, for  $\xi = 2\sqrt{\pi}$ , the self-similar solution reaches its maximum, where the curvature is 1.428 times its initial value  $\kappa_0$ . This coefficient is universal, being twice the maximum of the Fresnel sine integral. It characterizes the maximum of curvature in the intermediate regime (4). At later times,  $t \sim T$ , the superposition of the initial burst and its reflection on the clamped end further increase the curvature locally: numerically, we have found that the curvature reaches a value as high as  $3.12 \kappa_0$  for  $t = .144T$  and  $s = L$ , see Fig. 4.

The increase of  $\kappa(s, t)$  is rather unexpected. Indeed, one could imagine the motion of the rod to be essentially given by its fundamental mode of oscillation around the straight configuration:  $\kappa(s, t) \propto \kappa_0 \cos(2\pi t/T_{\text{free}})$ , where  $T_{\text{free}} = 1.79T$  is the period of free oscillations. This simple picture misleadingly suggests that, after the release of the rod, its curvature remains bounded by its initial value  $\kappa_0$  at all times, and reaches this value every half-period, when the rod is bent the other way around. In fact, the quick initial relaxation of the nonzero curvature  $\kappa(0, t)$  at the free end sends a burst of flexural waves, something that is not captured by the fundamental mode only. This burst is responsible for the subsequent increase of curva-

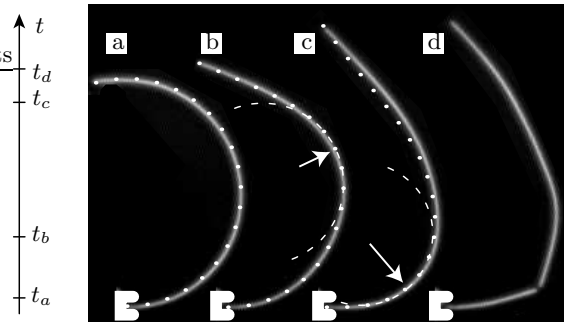


FIG. 3: A dry spaghetti can be broken by releasing one of its ends. The pasta is first bent into an arc of circle with a curvature slightly below its limit curvature. The lower end is clamped. The upper one is suddenly set free at time  $t_a = 0$ . Selected frames shot with a fast camera at 1000 Hz: (a) release  $t_a = 0$ , (b) intermediate frame  $t_b = 0.0159T$ , (c) frame just before rupture  $t_c = 0.0509T$ , and (d) after rupture  $t_d = 0.0596T$ . Numerical simulations based on the nonlinear Kirchhoff equations are superimposed, without any adjustable parameters: rod profile (dotted line) and osculating circle (dashed lines) at the point of largest curvature (arrow). Note that the rod breaks at the point of maximal curvature.

ture and leads to a cascade of cracks, as discussed below.

This analysis leads to a simple, although counter-intuitive prediction: releasing a bent pasta suffices to break it. This claim is indeed confirmed by the experiment presented in Fig. 3. A Barilla n° 1 dry spaghetti pasta of length  $L = 24.1$  cm was clamped and bent into an arc of circle, just below its limit curvature (by an angle  $\kappa_0 L = 195^\circ$ ). Digital photographs were acquired at 1000 frames per second using a fast camera while one end was released. The rod ruptured at a distance  $s = .76L$  of the free end, at a time  $t = 6.7$  ms after the release. From the period of free oscillations, we measured  $T = 114$  ms directly, hence a dimensionless fracture delay  $t/T = 58.5 \cdot 10^{-3}$ . A flexural wave travelling from top (released end) to bottom (clamped end) is clearly visible on the intermediate frames in the form of a local increase of curvature. The point of maximum curvature predicted by theory,  $(s/L)/\sqrt{t/T} = 2\sqrt{\pi}$ , is superimposed on the experimental snapshots along with the smallest osculating circle and the predicted rod configuration, without any adjustable parameters. The rod breaks exactly at the simulated maximum of curvature, as expected.

By repeating the experiment, we found that the failure delay and its location along the rod vary. Failure appears to be extremely sensitive to the initial curvature  $\kappa_0$  (rods that are closer to their limit curvature tend to break sooner after release, hence closer to released end) and probably also to the presence of defects. Twenty-five experiments were carried out with various pasta diameters (Barilla n° 1 with  $r_1 = .57$  mm and  $\gamma_1 = 0.521$  m<sup>2</sup>/s; Barilla n° 5 with  $r_5 = .84$  mm and  $\gamma_5 = 0.735$  m<sup>2</sup>/s; Barilla n° 7 with  $r_7 = .95$  mm and  $\gamma_7 = 0.82$  m<sup>2</sup>/s) and initial curvature (in the range  $9.7$  m<sup>-1</sup>– $15.3$  m<sup>-1</sup>), with

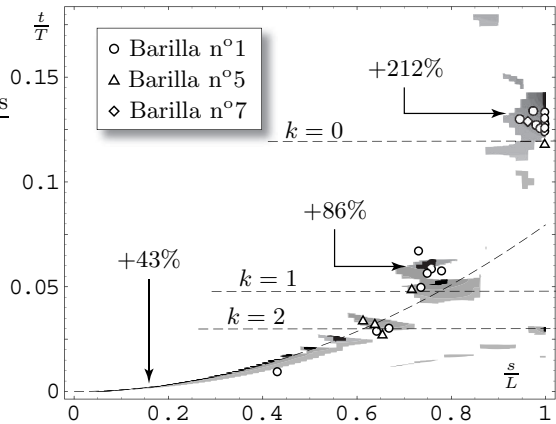


FIG. 4: Space-time diagram, in rescaled coordinates, of the breaking events obtained by repeating the experiment of Fig. 3 (data points) for different pasta radii and initial curvatures  $\kappa_0$ . The time and location of curvature records predicted by nonlinear numerical simulations for  $\kappa_0 L = \pi$  are shown in background, with no adjustable parameters: absolute records (black) and local ones (grey). Percentages show the relative increase of curvature  $\kappa/\kappa_0$  at selected points. Intersections of dashed parabola and horizontal lines labelled by  $k$  correspond to an approximate analytical prediction of breaking events (see main text).

$L$  around 24 cm. All the breaking events collapse onto a well-defined curve in a space-time diagram ( $s/L, t/T$ ), see Fig. 4. The curve of collapse can be predicted as follows. Assuming the rod has no defect, it breaks as soon as its limit curvature  $\kappa^*$  is reached somewhere. The first breaking event after the release must therefore correspond to the first time that  $|\kappa(s, t)|$  reaches the value  $\kappa^*$ . This means that breaking occurs necessarily at a point in the plane ( $s/L, t/T$ ) that is a *record* of curvature since the experiment started: for all  $s'$  and all  $t' < t$ ,  $|\kappa(s, t)| > |\kappa(s', t')|$ . This defines the so-called *absolute* curvature records. Under the opposite assumption that defects are important,  $\kappa^*$  becomes a function of  $s$  and rupture is simply expected to take place at a *local* curvature record, that is at a point ( $s, t$ ) such that  $|\kappa(s, t)| > |\kappa(s, t')|$  for all  $t' < t$  and same  $s$ . Global and local curvature records define a rather narrow region, shown in Fig. 4, onto which the experimental data points indeed collapse. These curvature records lie on a series of islands which can be interpreted as interference patterns between the incident and reflected waves. An analytical argument based on this remark shows that these islands lie at the intersection of the parabola  $(s/L)^2 = 4\pi t/T$  and the horizontal lines  $t/T = 1/(4\pi(k+q))$ , where  $k \geq 0$  is an integer and  $q \approx 2/3$  for clamped boundary conditions (dashed curves in Fig. 4). The collapse of the experimental data onto curvature records, without any adjustable parameters, confirms that this delayed rupture process is due to the flexural waves and the associated increase of curvature.

In the present analysis, we have only considered the

first breaking event after release, although multiple failures were commonly observed in experiments [18]. Secondary failure events are most likely described by the same theory, with a shorter timescale  $T$  (fragments are shorter), and with the additional difficulty that the initial curvature profile is not uniform. The present physical mechanism, based on flexural waves, for fragmentation of slender elastic bodies leads us to expect specific statistics for fragments sizes. Recall that the maximal curvature increases during the initial boundary layer,  $t \sim T_s$ , and later reaches a plateau,  $\kappa/\kappa_0 = 1.43$ . If the initial curvature is sufficiently close to the limit one, very early secondary breaking events should occur. Such events are too fast to be measured with our experimental setup but, nevertheless, we have often observed the ejection of tiny rod fragments, with typical size  $r$ . Such fragments, whose size and ejection velocity can probably be predicted by a boundary layer analysis, contribute in a non-trivial way to the statistics of fragments sizes. Data is being collected in order to test this hypothesis.

Contrary to the intuition that removing a loading decreases stresses and so cannot induce failure by itself, we have shown that rods can break just because they are released. When a bent rod reaches its limit curvature and breaks at a first point, a burst of flexural waves is sent through the newly formed fragments, which locally further increase the curvature. The limit curvature is therefore exceeded again at later time, allowing a cascading failure mechanism to take place. The cascade is limited by dissipation (propagation of transverse cracks, damping of flexural waves *e.g.* by visco-elastic effects in the material). The rupture delay  $t/T \simeq (s/L)^2/(4\pi)$  we derive here is singularly shorter than what would be conjectured from a crude analysis:  $t \sim T_{\text{free}} = 1.79 T$ . Finally, let us note that since this increase in curvature is described by a universal self-similar solution with no adjustable parameters it should be a fairly robust mechanism.

We are grateful to L. Lebon, D. Vallet and K. Liop for their help in setting up the experiments and to E. Villermaux and A. Belmonte for early communication of their preprint.

- 
- [1] N. F. Mott and E. H. Linfoot, Ministry of Supply Report No. AC3348 (1943), unpublished.
  - [2] D. E. Grady and M. E. Kipp, *Journal of Applied Physics* **58**, 1210 (1985).
  - [3] R. Englman, *J. Phys: Condens. Matter* **3**, 1019 (1991).
  - [4] L. Oddershede, P. Dimon, and J. Bohr, *Physical Review Letters* **71**, 3107 (1993).
  - [5] E. S. C. Ching, S. L. Lui, and K.-Q. Xia, *Physica A* **287**, 89 (2000).
  - [6] L. Griffith, *Can. J. Res.* **21**, 57 (1943).
  - [7] N. F. Mott, *Proc. Roy. Soc. London A* **189**, 300 (1947).
  - [8] J. R. Gladden, N. Z. Handzy, A. Belmonte, and E. Villier-

- maux (2004), preprint.
- [9] F. Wittel, F. Kun, H. J. Herrmann, and B. H. Kröplin, *Physical Review Letters* **93** (2004).
  - [10] D. A. Shockey, D. R. Curran, L. Seaman, J. T. Rosenberg, and C. F. Peterson, *Int. J. Rock. Mech. Min. Sci.* **11**, 303 (1974).
  - [11] P. Rosin and E. Rammler, *J. Inst. Fuel* **7**, 29 (1933).
  - [12] B. D. Coleman, E. H. Dill, M. Lembo, Z. Lu, and I. Tobias, *Arch. Rational Mech. Anal.* **121**, 339 (1993).
  - [13] L. D. Landau and E. M. Lifshitz, *Theory of Elasticity*, vol. 7 of *Course of Theoretical Physics* (Pergamon Press, Oxford, 1986), 3rd ed.
  - [14] S. S. Antman and L. S. Srubshchik, *Journal of Elasticity* **50**, 129 (1998).
  - [15] B. Audoly and S. Neukirch, in preparation.
  - [16] G. I. Barenblatt, *Similarity, self-similarity, and intermediate asymptotics* (Consultants Bureau, New York, 1979).
  - [17] For strongly bent rods the self-similar solution applies to a small region of size  $1/\kappa_0$ . Further away from the free end, nonlinearities modify the profile of the waves but their overall behaviour stays the same
  - [18] See online movies, <http://www.lmm.jussieu.fr/spaghetti>.